Proceedings of the 2005 IEEE
International Conference on Robotics and Automation
Barcelona, Spain, April 2005

Computation and Graphical Characterization of Robust Multiple-Contact Postures in 2D Gravitational Environments

Yizhar Or
Dept. of ME, Technion
izi@tx.technion.ac.il

Elon Rimon
Dept. of ME, Technion
rimon@tx.technion.ac.il

***Abstract*— This paper is concerned with the problem of identifying robust equilibrium postures of a planar mechanism supported by fixed frictional contacts in a two-dimensional gravitational field. The complex kinematic structure of the mechanism is lumped into a single rigid body, $\mathcal{B}$, with a variable center of mass. Inertial forces generated by moving parts of the mechanism are lumped into a neighborhood of wrenches centered at the nominal gravitational wrench. The identification of the robust equilibrium postures associated with a given set of contacts is reduced to the identification of center-of-mass locations that maintain equilibrium of $\mathcal{B}$ with respect to any wrench in the given neighborhood. The static response of $\mathcal{B}$ to an external wrench involves static indeterminacy and frictional constraints. The region of center-of-mass locations that generate equilibrium with respect to a particular external wrench is formulated as a linear programming problem, and a full graphical characterization is provided. The result is then generalized to robust equilibrium postures that resist a neighborhood of external wrenches. Finally, we present experimental results that validate the criteria for feasible equilibrium postures.**

I. Introduction

Quasistatic multi-legged locomotion in a gravitational environment requires criteria for identifying and computing equilibrium postures for the mechanism. This paper is concerned with the problem of identifying and computing the feasible equilibrium postures of a multi-limbed mechanism supported by a given set of frictional contacts in a two-dimensional gravitational field. In order to simplify the problem, we lump the complex kinematic structure of the mechanism into a single rigid body, $\mathcal{B}$, with a variable center of mass. Since free limbs of the mechanism must move during locomotion, we lump the inertial forces generated by its moving parts into a neighborhood of disturbance wrenches (i.e. forces and torques) centered at the nominal gravitational wrench. The identification of the feasible equilibrium postures associated with a given set of contacts and a given external wrench is reduced to the identification of center-of-mass locations that generate feasible equilibrium of $\mathcal{B}$, while satisfying the friction constraints at the contacts. However, in our case $\mathcal{B}$ is subjected to a neighborhood of external wrenches rather than a single wrench. Hence we introduce the notion of *robust equilibrium postures.* By definition, $\mathcal{B}$ is in a robust equilibrium posture with respect to a neighborhood of wrenches if the contacts supporting the object can statically resist the entire neighborhood of wrenches that act on $\mathcal{B}$. Based on this notion of robustness our objective is as follows. Given a set of contacts and a neighborhood of wrenches centered at the nominal gravitational wrench, we wish to identify all center-of-mass locations that guarantee a robust equilibrium posture of $\mathcal{B}$.

Some relevant literature about quasistatic multi-legged locomotion is as follows. Working with frictionless contacts, Mason et al. [9] introduced the idea of lumping the kinematic structure of a mechanism into a rigid body having the same contacts with the environment and a variable center of mass. They identified the statically stable postures of a mechanism supported by *frictionless* contacts in two and three-dimensions. A similar work with frictionless contacts has been conducted by Trinkle et al. [14] in the context of whole-arm manipulation. However, their approaches do not naturally generalize to frictional environments. Madhani and Dubowsky [6] describe a locomotion planner in the configuration space of a multi-limbed robot using nonlinear optimization over discrete nodes, considering friction constraints and static indeterminacy. Their method is based on the full configuration space of the robot, and hence is computationally intensive. Our objective is to characterize stable postures under the simple paradigm of rigid body with variable center-of-mass, assuming that the contact forces with the terrain are passive and cannot be measured or controlled. Erdmann et. al. [3] characterize the feasible center-of-mass positions for *two* frictional contacts in the context of nonprehensile palm manipulation. Bretl and Latombe [1] analyze the feasible center-of-mass positions for a 3-legged robot climbing on vertical walls with frictional supports. However, no previous work have formulated the feasible center-of-mass positions for a

0-7803-8914-X/05/$20.00 ©2005 IEEE.

general number of contacts, nor considered the practically important notion of robust equilibrium postures.

Our paper makes two contributions. First, it formulates the conditions for a multiple-contact feasible equilibrium posture as a linear programming problem in terms of $\mathcal{B}$'s center-of-mass location. This formulation applies both for a single and for a neighborhood of external wrenches. Second, it provides a full graphical characterization of the feasible equilibrium postures associated with a given set of contacts.

The structure of the paper is as follows. In the next section we formulate the feasible equilibrium region for multiple contacts and a single external wrench as a linear programming problem, and provide a graphical characterization of this region. In section III we generalize the results for a neighborhood of disturbance wrenches centered at the nominal gravitational wrench, compute the robust equilibrium region, and provide its graphical characterization. In section IV we present preliminary experimental results that validate the analytical criterion for a feasible equilibrium using a two-legged mechanism. Finally, the concluding section describes the need to account for dynamic ambiguity, and sketches extension of the results to robust 3D postures. Due to lack of space, proofs of the results in sections II and III are relegated to Ref. [11].

II. The Feasible Equilibrium Region

Given a planar body $\mathcal{B}$ with variable center-of-mass supported by k contacts against gravity, the *feasible equilibrium region* consists of the center-of-mass locations that can generate an equilibrium posture of $\mathcal{B}$. In this section we characterize the feasible equilibrium region under the following assumptions. First, the terrain is assumed to be *piecewise linear*. Second, $\mathcal{B}$ as well as the supporting contacts are assumed ideally rigid, and each support makes a point contact with $\mathcal{B}$. The latter assumption is relaxed in [11], where the results are generalized to contact patches. Third, we assume that the contact points of $\mathcal{B}$ with the terrain are known.

A. Basic Terminology

Let $x_1 \dots x_k$ denote the contact points supporting $\mathcal{B}$, and let x denotes $\mathcal{B}$'s center of mass expressed with respect to a fixed world frame. The forces acting on $\mathcal{B}$ at the contacts are denoted $f_1 \dots f_k$ and described with respect to the fixed world frame. The torque generated by f_i about $\mathcal{B}$'s center of mass is given by the scalar $\tau_i = (x_i - x)^T J^T f_i$, where $J = \begin{bmatrix} 0 & -1 \\ 1 & 0 \end{bmatrix}$. The gravitational force acting on $\mathcal{B}$ is denoted f_g. We also allow a disturbance wrench $(f_d, \tau_d) \in \mathbb{R}^2 \times \mathbb{R}$ acting on $\mathcal{B}$'s center-of-mass. Let $\boldsymbol{w} = (f_{ext}, \tau_{ext}) \in \mathbb{R}^2 \times \mathbb{R}$ denote the net external wrench acting on $\mathcal{B}$'s center-of-mass, then $f_{ext} = f_g + f_d$ such that $\|f_d\| \ll \|f_g\|$. Since f_g generates no torque about x, we have that $\tau_{ext} = \tau_d$. Note that the contact points x_i, as well as the normal direction to each contact, denoted n_i, are known.

When an external wrench $\boldsymbol{w} = (f_{ext}, \tau_{ext})$ acts on $\mathcal{B}$, the equilibrium condition is:

$$\begin{array}{l} f_1 + \cdots + f_k = -f_{ext} \\ (x_1 - x)^T J^T f_1 + \cdots + (x_k - x)^T J^T f_k = -\tau_{ext} \end{array} \quad (1)$$

Note that the contact forces are statically indeterminate for $k \geq 2$ contacts. Furthermore, the Coulomb friction law states that each contact force f_i must lie in a *friction cone,* denoted $\mathcal{C}_i$, in order to avoid sliding. Let μ be the coefficient of friction, and let f_i^n and f_i^t denote the normal and tangential components of f_i. Then $\mathcal{C}_i = \{f_i : |f_i^t| \leq \mu f_i^n, \ f_i^n \geq 0\}$. We also need the following equivalent terminology for $\mathcal{C}_i$. Let C_i^u and C_i^w denote unit vectors along the two edges of $\mathcal{C}_i$ (Figure 1(a)). Then the i^{th} friction cone is given by $\mathcal{C}_i = \{f_i^u C_i^u + f_i^w C_i^w : f_i^u, f_i^w \geq 0\}$. The *feasible equilibrium region*, denoted $\mathcal{R}(\boldsymbol{w})$, is the set of center-of-mass locations for which there exist feasible contact forces $f_i \in \mathcal{C}_i$ $(i = 1 \dots k)$ that satisfy the equilibrium condition (1).

B. Computation of the Feasible Equilibrium Region

We now show that the k-contact feasible equilibrium region $\mathcal{R}(\boldsymbol{w})$ where $\boldsymbol{w} = (f_{ext}, \tau_{ext})$ is an infinite strip parallel to f_{ext}, which can be computed as a linear programming problem. Each contact force can be written as $f_i = C_i^u f_i^u + C_i^w f_i^w$ where $f_i^u, f_i^w \geq 0$ and C_i^u, C_i^w are the edges of $\mathcal{C}_i$. First we write the equilibrium condition (1) in matrix form. Let us define the matrices

$$G_f = \begin{bmatrix} C_1^u & C_1^w & \cdots & C_k^u & C_k^w \end{bmatrix}_{2 \times 2k}$$

$$G_\tau = -\begin{bmatrix} x_1^T J C_1^u & x_1^T J C_1^w \cdots x_k^T J C_k^u & x_k^T J C_k^w \end{bmatrix}_{1 \times 2k}.$$

Then for $\vec{f} = (f_1^u \ f_1^w \cdots f_k^u \ f_k^w)$, the equilibrium condition (1) can be written as

$$\begin{bmatrix} G_f \\ G_\tau \end{bmatrix} \vec{f} = -\begin{pmatrix} f_{ext} \\ \tau(x) \end{pmatrix} \text{ and } \vec{f} \geq \vec{0}, \quad (2)$$

where $\tau(x) = x^T J^T f_{ext} + \tau_{ext}$ is the net torque generated by $\boldsymbol{w} = (f_{ext}, \tau_{ext})$ about the world frame origin. Note that x has been eliminated from the left side of (2). The following key theorem characterizes the feasible equilibrium region of $\boldsymbol{w}$ as a linear programming problem.

Theorem 1. *Let $\mathcal{B}$ be supported by k frictional contacts in a two-dimensional gravitational field, and be subjected to an external wrench $\boldsymbol{w} = (f_{ext}, \tau_{ext})$. Then the feasible equilibrium region $\mathcal{R}(\boldsymbol{w})$ is an* ***infinite strip*** *given by*

$$\mathcal{R}(\boldsymbol{w}) = \{x : \tau_{min} \leq x^T J^T f_{ext} + \tau_{ext} \leq \tau_{max}\}, \quad (3)$$

where τ_{min} and τ_{max} are obtained by solving the linear programming problems:

$$\tau_{min} = \min_{G_f \vec{f} = -f_{ext},\, \vec{f} \geq \vec{0}} \{-G_\tau \vec{f}\}$$
$$\tau_{max} = \max_{G_f \vec{f} = -f_{ext},\, \vec{f} \geq \vec{0}} \{-G_\tau \vec{f}\} \quad (4)$$

Proof sketch: Intuitively, the scalar $G_\tau \vec{f}$ is the net torque generated by the contacts in response to $\boldsymbol{w}$. The interval $[\tau_{min}, \tau_{max}]$ captures the range of torques that can be resisted by the contacts. Hence any center-of-mass location satisfying $\tau_{min} \leq \tau(x) \leq \tau_{max}$ allows the contacts to balance the net wrench acting on $\mathcal{B}$. □

Example 1: Figure 1(a) shows $\mathcal{R}(\boldsymbol{w})$ for two contacts using the nominal gravitational wrench $\boldsymbol{w} = (f_g, 0)$. Note that in this case $\mathcal{R}(\boldsymbol{w})$ is the vertical strip spanned by the polygon $\mathcal{C}_1 \cap \mathcal{C}_2$. The physical justification for this fact is discussed below.

C. Feasible Equilibrium Region for Multiple Contacts

In the following proposition we describe a significant structural property of $\mathcal{R}(\boldsymbol{w})$ for multiple contacts that will be useful in the ensuing graphical characterization of $\mathcal{R}(\boldsymbol{w})$.

Proposition II.1 ([11]). *Let $\mathcal{B}$ be supported by k frictional contacts in a two-dimensional gravitational field, and be subjected to an external wrench $\boldsymbol{w} = (f_{ext}, \tau_{ext})$. Then $\mathcal{R}(\boldsymbol{w})$ is the convex hull of the pairwise feasible equilibrium regions,*

$$\mathcal{R}(\boldsymbol{w}) = \mathsf{conv}\{\mathcal{R}_{ij}(\boldsymbol{w}) :\ 1 \leq i, j \leq k\}$$

where $\mathcal{R}_{ij}(\boldsymbol{w})$ is the feasible equilibrium region associated with the contacts x_i and x_j, and conv *denotes convex hull.*

The proposition implies that when constructing $\mathcal{R}(\boldsymbol{w})$ for multiple-contact postures, one simply needs to consider the feasible equilibrium strips generated by all pairs of contacts. Taking the convex hull of these parallel strips can be performed by simply identifying their leftmost and rightmost edges.

Example 2: Figure 1(b) shows the region $\mathcal{R}(\boldsymbol{w})$ for a six-contacts posture using the nominal gravitational wrench $\boldsymbol{w} = (f_g, 0)$. Computing the vertical strips $\mathcal{R}_{ij}(\boldsymbol{w})$ associated with all possible pairs of contacts, one can see that the leftmost edge is associated with $\mathcal{R}_{13}(\boldsymbol{w})$, while the rightmost edge is associated with $\mathcal{R}_{56}(\boldsymbol{w})$. Therefore, the feasible equlibrium region associated with all six contacts is simply the vertical strip between the leftmost and rightmost edges.

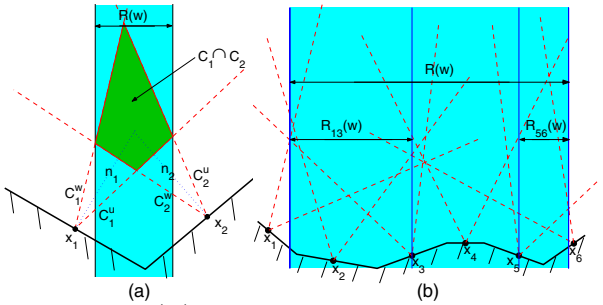

Fig. 1. $\mathcal{R}(\boldsymbol{w})$ for (a) two contacts and (b) six contacts.

D. Graphical Characterization of $\mathcal{R}(\boldsymbol{w})$

We now present a graphical characterization of the feasible equilibrium region $\mathcal{R}(\boldsymbol{w})$. Recall that $\mathcal{R}(\boldsymbol{w})$ for a k-contact posture can be obtained by first constructing the feasible equilibrium strips for all pairs of contacts, then taking the convex hull of these strips. Hence we focus on two-contact postures. First consider the nominal gravitational wrench $\boldsymbol{w}_o = (f_g, 0)$. The region $\mathcal{R}(\boldsymbol{w}_o)$ is a vertical strip that can be obtained by union and intersection of *five* strips, each having a distinct graphical interpretation. Before stating the procedure for constructing $\mathcal{R}(\boldsymbol{w}_o)$, we need the following notation. Recall that $\mathcal{C}_i$ denotes the friction cone at x_i. Let $\mathcal{C}_i^-$ denote the negative reflection of $\mathcal{C}_i$ about x_i. Let S_1^{++} denote the infinite vertical strip spanned by the polygon $\mathcal{C}_1 \cap \mathcal{C}_2$. Similarly, let $S_1^{+-}, S_1^{-+}, S_1^{--}$ denote the infinite vertical strips spanned by the polygons $\mathcal{C}_1^+ \cap \mathcal{C}_2^-$, $\mathcal{C}_1^- \cap \mathcal{C}_2^+$, and $\mathcal{C}_1^- \cap \mathcal{C}_2^-$ respectively. Note that some of these polygons and their associated strips may be empty. Finally, let S_2 denote the infinite vertical strip bounded by the contacts x_1 and x_2. The graphical construction of $\mathcal{R}(\boldsymbol{w}_o)$ is summarized in the following lemma.

Lemma II.2. *Let $\mathcal{B}$ be supported by two frictional contacts in a two-dimensional gravitational field, and be subjected to a gravitational wrench $\boldsymbol{w}_o = (f_g, 0)$. Then the feasible equilibrium region $\mathcal{R}(\boldsymbol{w}_o)$ is the infinite vertical strip given by*

$$\mathcal{R}(\boldsymbol{w}_o) = \big((S_1^{++} \cup S_1^{--}) \cap S_2\big) \cup \big((S_1^{+-} \cup S_1^{-+}) \cap \bar{S}_2\big),$$

where $\bar{S}_2$ is the complement of S_2 in $\mathbb{R}^2$.

Proof sketch: The proof is based on the fact that there are three external forces acting on $\mathcal{B}$: the gravitational force f_g at x, and the contact forces f_1 and f_2 at x_1 and x_2. The balance of moments implies that the three force lines intersect at a single point. Therefore, the line of f_g must pass through the intersection point of the lines of f_1 and f_2, which lies in $(\mathcal{C}_1 \cup \mathcal{C}_1^-) \cap (\mathcal{C}_2 \cup \mathcal{C}_2^-)$. The additional requirement of strip S_2 is implied by the fact that f_1 and f_2 must *positively* span $-f_g$. □

In the previous example of Figure 1(b), the strips S_1^{+-}, S_1^{-+} , and S_1^{--} are empty, and the strip S_1^{++}

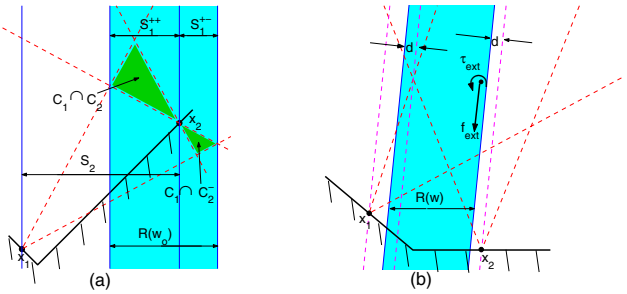

Fig. 2. Graphical characterization of $\mathcal{R}(\boldsymbol{w})$: (a) $\mathcal{R}(\boldsymbol{w}_o) = S_1^{++} \cup S_1^{+-}$, (b) $\mathcal{R}(\boldsymbol{w}) = S_1^{++} \cap S_2$ for a general wrench $\boldsymbol{w} = (f_{ext}, \tau_{ext})$.

is fully contained in S_2. Therefore $\mathcal{R}(\boldsymbol{w}_o)$ reduces to the strip S_1^{++}. In the non-symmetric example of Figure 2(a), $\mathcal{R}(\boldsymbol{w}_o)$ reduces to $S_1^{++} \cup S_1^{+-}$.

Note that even though $\mathcal{R}(\boldsymbol{w}_o)$ is a union of regions, it is always *a single connected strip* as asserted in Theorem 1. The graphical characterization of $\mathcal{R}(\boldsymbol{w}_o)$ is consistent with the characterization given in [3] in the context of object manipulation. It is also consistent with the analysis provided in [1] for 3-legged locomotion under gravity, and with the graphical methods in [7]. However, none of these works explicitly formulate $\mathcal{R}(\boldsymbol{w})$ for an arbitrary number of contacts. Furthermore, none of these works considers a general external wrench and neighborhoods of wrenches.

Extension to a general external wrench:

We now generalize the graphical characterization of $\mathcal{R}(\boldsymbol{w})$ to a general wrench $\boldsymbol{w} = (f_{ext}, \tau_{ext})$. When $\tau_{ext} = 0$, the force f_{ext} acts at x but is rotated about the vertical direction of f_g. Therefore the feasible equilibrium region is constructed by the same procedure described above, except that now the vertical strips S_1 and S_2 are rotated as to match the direction of f_{ext}. When $\tau_{ext} \neq 0$, the wrench $\boldsymbol{w}$ is equivalent to a pure force f_{ext} which acts with a perpendicular offset d from x, where $d = \tau_{ext}/\|f_{ext}\|$. Hence the strips S_1 and S_2 are rotated and parallel shifted by $-d$ as shown in the example of Figure 2(b), in which $\mathcal{R}(\boldsymbol{w})$ reduces to $S_1^{++} \cap S_2$.

The graphical characterization of $\mathcal{R}(\boldsymbol{w})$ for two contacts is extremely useful, since according to Proposition II.1 it allows construction of the k-contact feasible equilibrium region as the convex hull of the pairwise feasible equilibrium regions.

III. The Robust Equilibrium Region

So far we described the feasible equilibrium region for a particular external wrench $\boldsymbol{w}$ which is usually the nominal gravitational wrench. However, in practice one wishes to select *robust* postures that resist a set of external wrenches. Such sets originate mainly from small inertial forces generated by moving limbs of the mechanism during quasistatic locomotion. In this section we consider the computation of the *robust equilibrium region,* defined as $\mathcal{R}(\mathcal{W}) = \cap_{\boldsymbol{w} \in \mathcal{W}} \mathcal{R}(\boldsymbol{w})$, where $\mathcal{W}$ is a given neighborhood of disturbance wrenches centered at the nominal gravitational wrench. Any posture with center-of-mass in $\mathcal{R}(\mathcal{W})$ is robust in the sense that it generates a feasible equilibrium for *all* $\boldsymbol{w} \in \mathcal{W}$. First we describe a convenient parameterization for $\mathcal{W}$. Then we show how to compute the robust equilibrium region associated with $\mathcal{W}$ as a linear programming problem. Finally, we provide a graphical characterization of $\mathcal{R}(\mathcal{W})$.

A. Parametrization of the Wrench Neighborhood $\mathcal{W}$

A key fact is that equilibrium condition (1) is independent of the particular magnitude of the external wrench. We exploit this fact in the following wrench parametrization. Let (f_x, f_y) denote the horizontal and vertical coordinates of f_{ext}. Since $f_{ext} = f_g + f_d$ such that f_g is vertical and $\|f_d\| \ll \|f_g\|$, we may assume that $f_y \neq 0$. Thus we define *homogeneous coordinates* for wrench space as (p, q), where $p \triangleq f_x/f_y$ and $q \triangleq \tau_{ext}/f_y$. The (p, q) coordinates can be interpreted as follows. The nominal gravitational wrench, $\boldsymbol{w}_o = (f_g, 0)$, corresponds to $(p, q) = (0, 0)$. Any other wrench $\boldsymbol{w} = (f_{ext}, \tau_{ext}) \in I\!R^2 \times I\!R$ can be represented by its magnitude and its oriented line of action. The wrench's line of action is oriented along f_{ext}, and the horizontal distance of the line from $\mathcal{B}$'s center-of-mass is τ_{ext}/f_y. Hence p represents the orientation of the wrench's line of action, and q represents its horizontal distance from x. Using (p, q), we assume that $\mathcal{W}$ is a *rectangular neighborhood* given by $\mathcal{W} = \{(p, q) : \kappa_1 \leq p \leq \kappa_2, \nu_1 \leq q \leq \nu_2\}$, where κ_i and ν_i are given parameters for $i = 1, 2$.

B. Computation of the Robust Equilibrium Region

We now compute the robust equilibrium region $\mathcal{R}(\mathcal{W})$. Using the (p, q) parametrization for the external wrenches, the equilibrium condition (2) becomes

$$\begin{bmatrix} G_f \\ G_\tau \end{bmatrix} \vec{f} = - \begin{pmatrix} p \\ 1 \\ \tau(x) \end{pmatrix} \tag{5}$$

where $\vec{f} \geq \vec{0}$ and $\tau(x) = x^T J^T \begin{pmatrix} p \\ 1 \end{pmatrix} + q$.

The following theorem characterizes the robust equilibrium region $\mathcal{R}(\mathcal{W})$.

Theorem 2 ([11]). *Let $\mathcal{B}$ be supported by k frictional contacts in a two-dimensional gravitational field, and be subjected to a neighborhood $\mathcal{W} = [\kappa_1, \kappa_2] \times [\nu_1, \nu_2]$ of disturbance wrenches. Then the robust equilibrium region of $\mathcal{W}$ is the* **finite parallelogram** *given by*

$$\mathcal{R}(\mathcal{W}) = \big\{x : \\ \tau_{i,min} - \nu_1 \leq x^T J^T f_{ext}^i \leq \tau_{i,max} - \nu_2 \text{ for } i = 1, 2\big\},$$

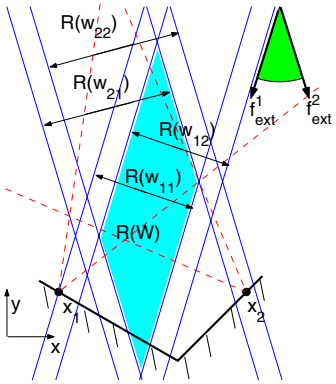

Fig. 3. The region $\mathcal{R}(\mathcal{W})$ for two contacts.

where $f^i_{ext} = (\kappa_i, 1)$*, and* $\tau_{i,min}, \tau_{i,max}$ *are obtained by solving the linear programming problems:*

$$\tau_{i,min} = \min_{G_f \vec{f} = -f^i_{ext},\ \vec{f} \geq \vec{0}} \{-G_\tau \vec{f}\}$$
$$\tau_{i,max} = \max_{G_f \vec{f} = -f^i_{ext},\ \vec{f} \geq \vec{0}} \{-G_\tau \vec{f}\} \text{ for } i = 1, 2.$$

Graphically, the parallelogram defined above is obtained by intersection of the strips $\mathcal{R}(\boldsymbol{w}_{ij})$, where $\boldsymbol{w}_{ij}$ are the external wrenches parametrized by $(p, q) = (\kappa_i, \nu_j)$ for $1 \leq i, j \leq 2$. The proof of Theorem 2 is in Ref. [11].

Example 3: In the example shown in Figure 3, two frictional contacts are supporting $\mathcal{B}$ with $\mu = 0.4$. We have chosen a rectangular wrench neighborhood $\mathcal{W} = [-\kappa, \kappa] \times [0, \nu]$ with $\kappa = 0.3$ and $\nu = \|x_2 - x_1\|/8$. The figure shows the strips $\mathcal{R}(\boldsymbol{w}_{ij})$ associated with the vertices of $\mathcal{W}$. The shaded region $\mathcal{R}(\mathcal{W})$ is the parallelogram obtained by intersection of these four strips.

IV. Experimental Results

In this section we present results of preliminary experiments that test the static equilibrium of a two-legged mechanism in frictional contact with a variable terrain, under disturbance forces. The goal of these experiments is to validate the static analysis of feasible equilibrium criteria in a frictional environment, under gravity and disturbance forces.

The experimental system shown in figure 4 consists of a two-legged mechanism prototype made of Aluminium, whose center-of-mass position can be changed by mounting a heavy weight on a vertical bar with an adjustable angle. The mechanism is placed on a rigid V-shaped terrain of two segments with adjustable slopes. A horizontal force is applied on the mechanism by a variable weight hung on a string through a pulley. In our experiment the mechanism is positioned on a symmetric V-shaped terrain with slope angles of $\alpha = 26.7^o$. The external horizontal force is then gradually increased until reaching a critical value at which the contacts break or slip. The critical force is recorded, and this process is

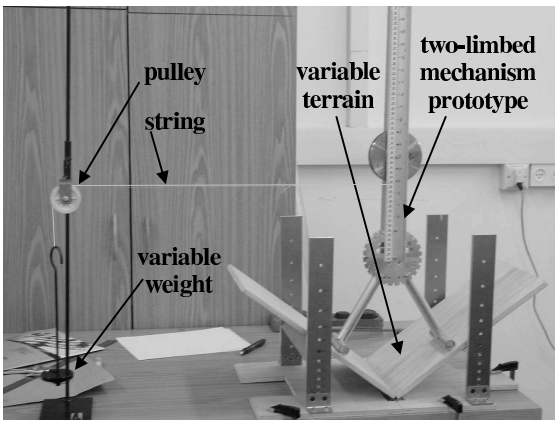

Fig. 4. Experimental setup of a two-legged mechanism prototype.

repeated for different heights of the horizontal force's application point. As a preliminary step, the coefficient of friction was experimentally determined to be $\mu = 0.25$ with a standard deviation of $\pm 6.5\%$.

In order to analyze the problem and predict the expected results, let us denote the horizontal distance between the contacts as l, and the vertical distance of the horizontal force application point from the contact points as h. Also, let f_g be the gravitational force, which is the mechanism's constant weight. The external horizontal force, denoted f_d, is variable. The total applied force is rotated by the angle $\beta = \tan^{-1}(f_d/f_g)$ about the vertical direction, where f_g and f_d are now scalars. Although the static contact reaction forces are indeterminate, the two possible critical cases of contact breakage or slippage are determinate and can be obtained graphically as follows. The first critical case occurs when the action line of the net external force intersects the contact point x_2, as shown in Figure 5(a). In this case the contact reaction force at x_1 vanishes, resulting in contact breakage at x_1 and rolling about x_2. The corresponding critical force angle is $\beta_1 = tan^{-1}(l/2h)$. The second critical case occurs when the action line of the net external force intersects the point p_{uu}, as shown in Figure 5(b). In this case the contact reaction forces lie on the edges of their respective friction cones, and sliding starts at both contacts. Using geometric relations, the corresponding critical force angle is $\beta_2 = tan^{-1}(sin2\gamma/(2hsin2\gamma/l - cos2\alpha - cos2\gamma))$, where $\gamma = \tan^{-1}(\mu)$. The critical force f_d for which the equilibrium conditions are violated, is given by $f_d = f_g tan(\beta)$, where $\beta = \min\{\beta_1, \beta_2\}$.

The experimental results are presented in Figure 6. For each force application height h, five experiments were conducted and the average critical force f_d was measured with its corresponding angle β. In order to present a linear relationship, we plot $cot(\beta)$ as a function of h. The dashed and solid lines are $cot(\beta_1)$ and $cot(\beta_2)$, computed analytically as a function of h. Since $\beta = \min\{\beta_1, \beta_2\}$, the experimental results were expected to

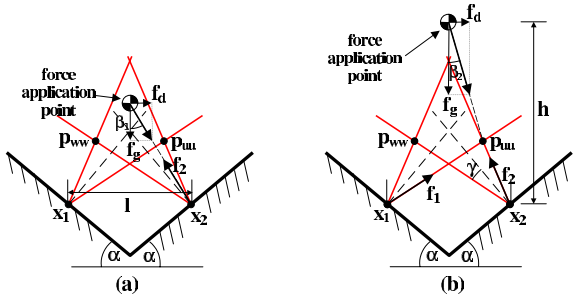

Fig. 5. Graphical characterization of critical horizonal force: (a) $f_d = f_g tan(\beta_1)$ and (b) $f_d = f_g tan(\beta_2)$.

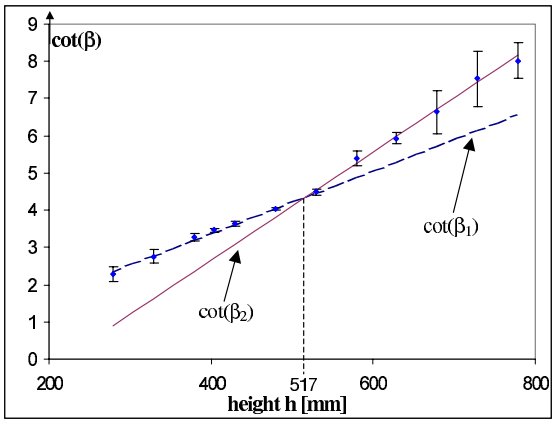

Fig. 6. Experimental (dots) and theoretical (solid and dashed lines) results of $cot(\beta)$ as a function of h.

follow the line of $cot(\beta_1)$ up to $h = 517mm$, then follow the line of $cot(\beta_2)$ for $h > 517mm$. The experimental results are marked as dots, with error bars of two standard deviations. One can see a close matching of the predicted behavior and the experimental results. The close matching corroborates our analytical equilibrium conditions based on Coulomb's friction law.

V. Concluding Discussion

We characterized the feasible equilibrium region associated with a given set of frictional contacts in a planar gravitational field. The computation of the feasible equilibrium region was formulated as a linear programming problem, and a graphical characterization of this region was provided as well. The results were then generalized to guarantee postures which are robust with respect to a neighborhood of disturbance wrenches. Finally, we presented preliminary experimental results verifying the analytical criteria employed in the analysis.

We now briefly discuss generalization of the results to three dimensions, and dynamic analysis of posture stability. In a 3D posture each contact generates a reaction force f_i with one normal component f_i^n, and *two* tangential components f_i^t and f_i^s. According to Coulomb's friction law, the friction cone is now $\mathcal{C}_i = \{f_i : \sqrt{(f_i^t)^2 + (f_i^s)^2} \leq \mu f_i^n \text{ and } f_i^n \geq 0\}$. Since the 3D frictional constraints are quadratic and convex, the equilibrium condition can be formulated as a linear matrix inequality (LMI) problem in $I\!R^{3k+2}$ [4]. The 3D feasible equilibrium region associated with a given set of contacts and an external wrench is now an infinite *prism* whose axis is parallel to f_{ext} .

Finally, one must recall that the criterion of feasible equilibrium is basically static. In order to fully characterize a candidate posture, one must also consider its *dynamic stability*. For dynamic analysis, one must consider the dynamic response at the contacts, and ensure that the contacts would not break, roll, or slip in response to small perturbations. A key problem is that rigid-body dynamics with frictional contacts can be ambiguous [5], [8], and the dynamic analysis must include all possible contact modes [13], [2]. A complete dynamic analysis, based on Trinkle's criterion of *strong stability* [12] will be presented in a paper currently under preperation. The reader is referred to [10] for preliminary work on this subject.

References

[1] T. Bretl, S. Rock, and J.C. Latombe. Motion planning for a three-limbed climbing robot in vertical natural terrain. In *IEEE Int. Conf. on Robotics and Automation*, pages 2946– 2953, 2003.

[2] P. Dupont. The effect of Coulomb friction on the existence and uniqueness of the forward dynamics problem. In *IEEE Int. Conf. on Robotics and Automation*, pages 1442– 1447, 1992.

[3] M. A. Erdmann. An exploration of nonprehensile two-palm manipulation. *Int. J. of Robotics Research*, 17(5):485–503, 1998.

[4] Li Han, J.C. Trinkle, and Z.X. Li. Grasp analysis as linear matrix inequality problems. *IEEE Trans. on Robotics and Automation*, 16(6):663–674, 2000.

[5] P. Lotstedt. Coulomb friction in two-dimensional rigid body systems. *Zeitschrift fur Angewandte Mathematik und Mechanik*, 61:605–615, 1981.

[6] A. Madhani and S. Dubowsky. Motion planning of mobile multi-limb robotic systems subject to force and friction constraints. In *IEEE Int. Conf. on Robotics and Automation*, pages 233–239, 1992.

[7] M.T. Mason. Two Graphical Methods for Planar Contact Problems. IEEE/RSJ International Conference on Intelligent Robots and Systems, Intelligence for Mechanical Systems, pages 443–448, 1991.

[8] M. T. Mason and Y. Wang. On the inconsistency of rigid-body frictional planar mechanics. In *IEEE Int. Conf. on Robotics and Aut.*, pages 524–528, 1988.

[9] R. Mason, J. W. Burdick, and E. Rimon. Stable poses of three-dimensional objects. In *IEEE Int. Conf. on Robotics and Automation*, pages 391–398, 1997.

[10] Y. Or and E. Rimon. Robust multiple contact postures in a two-dimensional gravitational field. In *IEEE Int. Conf. on Robotics and Automation*, pages 4783–4788, 2004.

[11] Y. Or and E. Rimon. Computation and graphic characterization of robust multiple-contact postures in 2D gravitational environments. Tech. report, Dept. of Mechanical Engineering, Technion, http://robots.technion.ac.il, August 2004.

[12] J. S. Pang and J. C. Trinkle. Stability characterizations of fixtured rigid bodies with coulomb friction. In *IEEE Int. Conf. on Robotics and Automation*, pages 361–368, 2000.

[13] V. T. Rajan, R. Burridge, and J. T. Schwartz. Dynamics of rigid body in frictional contact with rigid walls. In *IEEE Int. Conf. on Robotics and Automation*, pages 671–677, 1987.

[14] J. C. Trinkle, A. O. Farahat, and P. F. Stiller. First-order stability cells of active multi-rigid-body systems. *IEEE Trans. on Robotics and Automation*, 11(4):545–557, 1995.